0026-895X/01/6003-440–449$3.00
MOLECULAR PHARMACOLOGY
Copyright © 2001 The American Society for Pharmacology and Experimental Therapeutics
Mol Pharmacol 60:440–449, 2001

Vol. 60, No. 3
674/923909
Printed in U.S.A.

Differential Cell Death Induced by Salsolinol with and without Copper: Possible Role of Reactive Oxygen Species

HYUN-JUNG KIM, YUNJO SOH, JUNG-HEE JANG, JEONG-SANG LEE, YOUNG J. OH, and YOUNG-JOON SURH

College of Pharmacy, Seoul National University, Seoul, Korea (H.-J.K., J.-H.J., J.-S.L., Y.-J.S.); Department of Neuroscience, Graduate School of East-West Medical Science, Kyung Hee University, Youngin-city, Kyungki-do, Korea (Y.S.); and Department of Biology, Yonsei University, Seoul, Korea (Y.J.O.)

Received November 1, 2000; accepted May 11, 2001

This paper is available online at http://molpharm.aspetjournals.org

ABSTRACT

Salsolinol (SAL), a novel dopaminergic catechol tetrahydroisoquinoline neurotoxin, has been speculated to contribute to the etiology of Parkinson's disease and neuropathology of chronic alcoholism. Our previous studies have demonstrated that SAL induces strand scission in øX174 supercoiled DNA and oxidative base modification in calf thymus DNA in the presence of cupric ion. We now report that treatment of rat pheochromocytoma (PC12) cells with SAL causes reduced viability, which was exacerbated by Cu^{2+}. The copper chelator bathocuproinedisulfonic acid ameliorated cytotoxicity induced by SAL and Cu^{2+}. *N*-Acetyl-L-cysteine and reduced glutathione protected against SAL- plus Cu^{2+}-mediated PC12 cell death. Cells exposed to SAL underwent apoptosis, as revealed by characteristic morphological and biochemical changes. SAL treatment resulted in increased levels of Bax with a concomitant decrease in expression of Bcl-x_L. Furthermore, SAL rapidly activated c-Jun N-terminal kinase, whereas the activity of extracellular signal-regulated protein kinase remained unchanged. Transfection with Bcl-x_L or Bcl-2 led to protection against SAL-mediated PC12 cell death. Although SAL alone could cause apoptotic death in PC12 cells, cells treated with SAL together with Cu^{2+} became necrotic. Cells exposed to both SAL and Cu^{2+} exhibited higher levels of intracellular reactive oxygen species, malondialdehyde, and 8-oxo-7,8-dihydro-2′-deoxyguanosine than did those treated with SAL alone. These results suggest that copper accelerates redox cycling of SAL, leading to massive production of reactive oxygen species, which can divert the SAL-induced cell death to necrosis.

Salsolinol (SAL; 1-methyl-6,7-dihydroxy-1,2,3,4-tetrahydroisoquinoline; structure shown in Fig. 1) is one of the dopaminergic tetrahydroisoquinoline neurotoxins. The local concentration of this isoquinoline derivative increases in rat brain during ethanol intoxication (Collins, 1982; Myers et al., 1985), which is assumed to result from the Pictet-Spengler condensation reaction between dopamine and acetaldehyde, a product of ethanol metabolism (Collins, 1982). Urinary concentrations of SAL were found to be significantly higher in chronic alcoholics than in nonalcoholic control subjects (Collins et al., 1979; Adachi et al., 1986). Moreover, alcoholics exhibit significantly elevated plasma levels of SAL sulfate (Rommelspacher et al., 1995). The influence of ethanol on the SAL excretion in healthy subjects was also investigated (Haber et al., 1996). The results of this study indicate that urinary SAL output was augmented by the intake of ethanol. In addition, SAL was detected in lumbar cerebrospinal fluid of Parkinsonian patients (Moser and Kompf, 1992). However, the biochemical and molecular mechanisms of neurotoxicity exerted by SAL remain poorly understood.

It has been recognized that certain transition metal ions, such as Cu^{2+}, can stimulate the redox cycling of catechols (see below). Copper is an essential trace element that is present in many tissues of human body. Besides forming an essential redox-active center in many enzymes and metalloproteins, copper is found in nuclei in association with chromosomal DNA (Bryan et al., 1981). Like iron, copper plays an important role in the production of highly reactive hydroxyl radicals through the Fenton reaction. There is evidence that reactivity or toxicity of certain chemicals increases in the presence of cupric ion. For instance, glucasone was reported to be cytotoxic toward Chinese hamster lung V79 cells when cupric ion was added to the medium (Nakayama et al., 1992).

This work was supported by the Academic Research Fund (GE 997-019-D0008) awarded to Y.-J.S. from the Ministry of Education, Republic of Korea. This manuscript was prepared from a dissertation by H.-J.K. in partial fulfillment of the requirement for a Masters of Science at Seoul National University. Y.S. and J.-H.J. contributed equally to this work.

ABBREVIATIONS: SAL, salsolinol; ROS, reactive oxygen species; 6-OHDA, 6-hydroxydopamine; MAP, mitogen-activated protein; JNK, c-Jun-N-terminal kinase; ERK, extracellular signal-mediated protein kinase; BCS, bathocuproinedisulfonic acid; NAC, *N*-acetyl-L-cysteine; GSH, reduced glutathione; MTT, 3-(4,5-dimethylthiazol-2-yl)-2,5-diphenyltetrazolium bromide; DAPI, 4′,6-diamidino-2-phenylindole; PBS, phosphate-buffered saline; TUNEL, terminal deoxynucleotidyl transferase-mediated dUTP-X nick-end labeling; DCF-DA, 2′,7′-dichlorodihydrofluorescein diacetate; MDA, malondialdehyde; 8-oxo-dGuo, 8-oxo-7,8-dihydro-2′-deoxyguanosine; dGuo, deoxyguanosine; HPLC, high-performance liquid chromatography.

Uric acid, when coincubated with cupric ion, caused breakage in calf thymus DNA and also converted supercoiled plasmid pBR322 DNA to a relaxed open circular form (Shamsi and Hadi, 1995). During uric acid plus Cu^{2+}-mediated DNA strand scission, reactive oxygen species (ROS), such as hydroxyl radicals, could be generated (Shamsi and Hadi, 1995). Quercetin induced DNA strand scission in the presence of Cu^{2+} (Fazal et al., 1990), which was shown to be mediated by ROS. Copper-dependent DNA-damaging activity of quercetin was attenuated by radical scavengers, such as iodide, mannitol, and formate, and also by such antioxidant enzymes as superoxide dismutase and catalase. The catechol estrogen 2-hydroxyestradiol is also oxidized to generate ROS in a copper-dependent manner (Li et al., 1994). The dopaminergic neurotoxin 6-hydroxydopamine (6-OHDA) is an unstable compound, which autoxidizes readily to form quinoid products (Graham et al., 1978; Nappi and Vass, 1994). Cupric ion was found to accelerate the autoxidation of 6-OHDA (Heikkila and Cabbat, 1978; Levay et al., 1997). The 6,7-dihydroxy functional group of SAL constitutes a catechol moiety and may also undergo oxidation to form quinoid products with concomitant generation of ROS.

Our previous studies have demonstrated that SAL in the presence of cupric ion causes strand breakage in øX174 or pBR322 supercoiled DNA and oxidative base modification in calf thymus DNA (Kim et al., 1997; Jung and Surh, 2001). Moreover, rat pheochromocytoma (PC12) cells exposed to SAL plus Cu^{2+} were less viable compared with cells treated with SAL alone. In an attempt to elucidate the mechanisms underlying Cu^{2+} enhancement of SAL-mediated cytotoxicity in PC12 cells and to investigate the possible roles of ROS in this process, we have initially assessed the accumulation of ROS in PC12 cells treated with SAL in the absence or presence of Cu^{2+}. We also examined the characteristics of cell death induced by SAL alone or SAL plus Cu^{2+} by using biochemical and morphological endpoints. In addition, we have determined the possible involvement of selected mitogen-activated protein (MAP) kinases, such as c-Jun-*N*-terminal kinase (JNK) and extracellular signal-mediated protein kinase (ERK), in mediating SAL-induced PC12 cell death.

Experimental Procedures

Materials. SAL, cupric sulfate ($CuSO_4 \cdot 5H_2O$), poly-D-lysine, bathocuproinedisulfonic acid (BCS) disodium salt, *N*-acetyl-L-cysteine (NAC), reduced glutathione (GSH), *N,N*-dimethylformamide, and 3-(4,5-dimethylthiazol-2-yl)-2,5-diphenyltetrazolium bromide (MTT) were purchased from Sigma (St. Louis, MO). N-2 supplement, F-12 nutrient mixture, Dulbecco's modified Eagle's medium, Hanks' balanced salt solution, horse serum, and fetal bovine serum were provided from Invitrogen (Carlsbad, CA). Low-melting agarose was a product of Amresco (Solon, OH). 3,3′-Diaminobenzidine and 4′,6-diamidino-2-phenylindole (DAPI) were supplied from DAKO (Glostrup, Denmark) and Partec (Muenster, Germany), respectively.

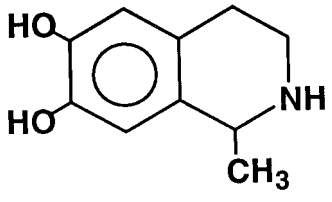

Fig. 1. Chemical structure of SAL.

2′,7′-Dichlorodihydrofluorescein diacetate (DCF-DA) was obtained from Molecular Probes (Eugene, OR). An in situ apoptosis detection kit was purchased from Oncor (Gaithersburg, MD). All other chemicals used were of analytical grade or the highest grade available.

Determination of Cell Viability. PC12 cells were initially plated at a density of 2×10^6 and 4×10^4 cells in 50 μg/ml poly-D-lysine–coated culture dishes and 48-well plates, respectively (or 2×10^5 cells/24-wells) and maintained at 37°C in a humidified atmosphere of 10% CO_2/90% air in Dulbecco's modified Eagle's medium, supplemented with 10% horse serum and 5% fetal bovine serum for 2 days. Cells were subsequently switched to serum-free N-2-defined medium containing SAL with and without Cu^{2+}. Cell viabilities were determined by the conventional MTT dye reduction assay. After incubation, cells were treated with the MTT solution (final concentration, 1 mg/ml) for 2 h. Formazan grains formed in intact cells were solubilized with 20% SDS in 50% aqueous *N,N*-dimethylformamide, and absorbance at 540 to 595 nm was measured with a microplate reader (Molecular Devices, Menlo Park, CA).

The trypan blue exclusion assay is based on the capability of viable cells to exclude the dye. Because apoptotic cells retain their membrane integrity, cells in the early stages of apoptosis retain their ability to exclude the dye, whereas necrotic cells with damaged plasma membrane fail to do so. An equal volume of 0.4% trypan blue staining solution was added to 48-well plated cells, and after 5 min, cells were loaded into a hemocytometer and counted for the dye uptake.

Nuclear Staining. PC12 cells (4×10^4) were maintained in poly-D-lysine–coated chamber slides. Cells treated with SAL alone or SAL plus cupric sulfate (100 μM) were washed with phosphate-buffered saline (PBS) twice and then fixed with 10% neutral buffered formalia (Sigma). Cells were stained with 5 μg/ml DAPI for 5 min, washed with PBS once, and mounted with 90% glycerol. Cells were observed under an UV illumination microscope.

DNA Fragmentation. PC12 cells (10^7) were harvested and washed twice with ice-cold Hanks' balanced salt solution. Cells were lysed in a solution consisting of 0.5% Triton X-100, 5 mM Tris-HCl buffer, pH 7.4, and 20 mM EDTA for 20 min at 4°C. After centrifugation at 15,000 rpm for 15 min, supernatants were extracted with phenol/chloroform/isoamyl alcohol (v/v, 25:24:1), and DNA was precipitated with ice-cold ethanol. Soluble DNA obtained was incubated with DNase-free RNase, and two-thirds of each sample was subjected to 1.8% agarose gel electrophoresis. Gel was subsequently stained with ethidium bromide, visualized on a transilluminator, and photographed using Polaroid 667 film (Polaroid, Cambridge, MA).

Terminal Deoxynucleotidyl Transferase-Mediated dUTP-X Nick-End Labeling (TUNEL) Assay. This assay was conducted following the instructions for the in situ apoptosis detection kit supplied from Oncor. Briefly, PC12 cells (5×10^7 in culture dishes) treated with SAL, Cu^{2+}, or both were fixed in 1 ml of 4% neutral buffered formalin for 10 min at room temperature. An aliquot (100 μl) of each sample was then placed on the slide glass and dried for 1 h. After washing twice with PBS for 5 min at room temperature using a Coplin jar, each sample was exposed to 2.0% hydrogen peroxide in PBS for 5 min at room temperature to quench endogenous peroxidase. After gentle removal of excess liquid, specimens were treated with two drops of equilibration buffer for 15 s and then incubated with terminal deoxynucleotidyl transferase in a humidified chamber at 37°C for 1 h. The reaction was stopped by washing samples with the buffer supplied. Specimens were then incubated for another 30 min with two drops of antidigoxigenin-peroxidase at room temperature. After washing with PBS, cells were stained with 3,3′-diaminobenzidine for 5 min. Cells were also counterstained with methyl green for 10 min at room temperature. After cells were rinsed with 100% butanol and xylene, they were mounted with 90% glycerol.

Transmission Electron Microscopy. Cultures were washed with PBS, pH 7.4, 3 times and fixed in 4% paraformaldehyde and 5%

glutaraldehyde in cacodylate buffer, pH 7.4, for 2 h. After washing with cacodylate buffer 3 times, cells were postfixed in 2% osmium tetroxide in *S*-collidine buffer, pH 7.4, for 1 h. Samples were then washed with distilled water 3 times. After staining en bloc in 0.4% uranyl acetate for 1 h, cultures were dehydrated serially with increasing concentrations of ethanol and embedded in Epon resin (EMbed-812, Electron Microscopy Sciences, Fort Washington, PA). Ultrathin sections (70 nm) were prepared using Reichert-Jung Ultracut J, picked up on collodion-coated copper grids, and double-stained with 0.4% uranyl acetate and 2% lead citrate. After carbon coating using a vacuum evaporator (JEE-4X; JEOL, Tokyo, Japan), the samples were photographed on a JEOL 1200EX-II electron microscope at 80 kV.

Measurement of Intracellular Peroxide. To monitor net intracellular accumulation of hydroperoxides after exposure to SAL alone or SAL plus Cu^{2+}, DCF-DA was used. DCF-DA is a membrane permeable nonfluorescent compound that, in the presence of peroxides, is converted intracellularly to the fluorescent 2′,7′-dichlorofluorescein. Cells were rinsed with Krebs-Ringer solution, and 10 μM DCF-DA was loaded. After 15 min of incubation at 37°C, cells were examined under a confocal microscope equipped with an argon laser (488 nm, 200 mW). After taking photographs, cells were lysed with dimethyl sulfoxide, and the intensities of fluorescence were measured using a spectrofluorometer (model 450; Turner Designs, Sunnyvale, CA). To quantify oxidant generation in response to SAL or SAL plus Cu^{2+}, total ROS generation (basal + increase) was divided by basal ROS generation. Changes in fluorescence intensity are expressed as a percentage of the control.

Measurement of Oxygen Consumption. The rate of oxygen consumption was measured with a biological oxygen monitor equipped with a Clark-type oxygen electrode (YSI-5300; YSI, Inc., Yellow Spring, OH), as described by Li et al. (1994). One minute after air saturation, 250 μM SAL in *N,N*-dimethylformamide was injected, 250 mM cupric sulfate or PBS was added, and oxygen consumption was monitored for up to 12 min.

Determination of Malondialdehyde (MDA) Formation. The formation of MDA, a substance produced during lipid peroxidation, was determined by using the commercially available colorimetric assay kit (BIOXYTECH LPO-586; OXIS Research, Inc., Portland, OR). After exposure to 100 μM SAL alone or in combination with the same concentration of Cu^{2+} at 37°C for 24 h, PC12 cells were harvested and homogenized in 20 mM Tris-HCl buffer, pH 7.4, containing 0.5 mM butylated hydroxytoluene to prevent sample oxidation. After centrifugation, 3.25 volumes of diluted R1 reagent (10.3 mM *N*-methyl-2-phenylindole in acetonitrile) was added to the supernatant, followed by gentle vortex mixing. After addition of 0.75 volumes of 37% HCl, the mixtures were incubated at 45°C for 60 min. After cooling and centrifugation, the absorbance of the clear supernatant was read at 590 nm. The protein concentration was determined using the bicinchoninic acid protein assay kit (Pierce, Rockford, IL).

Immunoperoxidase Staining for 8-Hydroxydeoxyguanosine. 8-Oxo-7,8-dihydro-2′-deoxyguanosine (8-oxo-dGuo) has been recognized as a useful marker for estimating oxidative DNA damage produced by ROS. For detection and quantitation of 8-oxo-dGuo formed in PC12 cells, we have adopted the immunoperoxidase method with a monoclonal antibody recognizing 8-oxo-dGuo (Yarborough et al., 1996). Stained cells were analyzed under a light microscope and photographed. The relative intensity of nuclear staining was measured by examining the average number of randomly selected cells in four different microscopic areas.

HPLC Analysis of 8-oxo-dGuo Formation. DNA was isolated from the cell lysates, as described in the protocol for the DNA extractor WB kit (Wako Pure Chemicals, Nagoya, Japan). Isolated DNA samples were subjected to hydrolysis in 100 μl of 20 mM sodium acetate buffer, pH 5.0, using 3 μl of 5 mg/ml nuclease P_1 (Sigma) at 37°C for 30 min. After the pH of the solution was adjusted to 8.0 by the addition of 10 μl of 1 M Tris-HCl buffer, pH 8.5, 2 units of calf intestine alkaline phosphatase was added, and the incubation was continued at 37°C for additional 1 h. The reaction was terminated by the addition of 250 mM sodium acetate, pH 5.0, and 4 mM EDTA. The hydrolysates were centrifuged at 15,000*g* for 30 min at 4°C and analyzed by HPLC coupled with the electrochemical detector (ESA, Inc., Chelmsford, MA) using a C_{18} reverse-phase column (4 μm; 3.9 × 150 mm). Products were eluted with 10% methanol in 50 mM sodium phosphate buffer, pH 5.0, at a flow rate of 0.5 ml/min. The amount of 8-oxo-dGuo and dGuo were calculated from the corresponding peak areas, and the results were expressed as the ratio of 8-oxo-dGuo to 10^5 dGuo.

Western Blot Analysis of Bcl-x_L and Bax. After treatment, cells were harvested by shaking and centrifugation (300*g* for 5 min). Collected cells were washed simultaneously with PBS by consecutive resuspension of pellets. After centrifugation, cell lysis was carried out at 4°C by vigorous shaking for 15 min in lysis buffer (50 mM Tris-HCl, pH 8.0, 2 mM EDTA, and 1% Triton X-100 with a protease inhibitor cocktail tablet). Nuclei and unlysed cellular debris were removed by centrifugation at 15,000 rpm for 15 min. Protein samples (35 μg) were solubilized with SDS-polyacrylamide gel electrophoresis sample loading buffer and electrophoresed on a 15% SDS-polycrylamide gel. Proteins were transferred to polyvinylidene difluoride blots for 1 h at 4°C. Filters were blocked for 1 h at room temperature in fresh blocking buffer prepared with 0.05% Tween 20 in PBS, pH 7.4, containing 3% nonfat dry milk. Dilutions of primary (mouse anti-Bcl-x_L or rabbit anti-Bax) and horseradish-conjugated secondary antibodies were made in 0.05% Tween 20 in PBS, pH 7.4, and incubation of blots was performed for 1 h at room temperature. The transferred proteins were visualized with an enhanced chemiluminescence detection kit (Amersham Pharmacia Biotech, Inc., Piscataway, NJ), according to the manufacturer's instructions.

Immunocomplex Kinase Activity Assay. After treatment for various time intervals, cells were harvested and homogenized in ice-cold lysis buffer containing 20 mM HEPES, pH 7.4, 150 mM NaCl, 1 mM EDTA, 1 mM EGTA, 1% Triton X-100, 2.5 mM sodium pyrophosphate, 0.5 mM dithiothreitol, 12.5 mM β-glycerophosphate, 1 mM Na_3VO_4, and 1 μg/ml leupeptin. Cell debris and particulate fractions were removed by centrifugation at 14,000*g* for 10 min at 4°C. The catalytic activity of JNK1 or ERK in the remaining soluble fraction (200 μg/reaction) was measured after immunoprecipitation using the respective antibodies (a mouse monoclonal antibody for JNK1 or a polyclonal antibody for ERK2) according to the published method (Soh et al., 2000). The kinase reaction buffer contained 20 mM HEPES, pH 7.4, 1 mM β-glycerophosphate, 7.5 mM $MgCl_2$, 0.5 mM EGTA, 0.5 mM NaF, 0.5 mM Na_3VO_4, 0.05 mg/ml substrate protein, 20 mM ATP, and 2 μCi of [γ-^{32}P]ATP. Purified glutathione *S*-transferase-activating transcription factor-2 fusion protein was used as a substrate for JNK1 and myelin basic protein for ERK. The reaction was initiated by the addition of radiolabeled ATP to the reaction mixture. After incubation for 30 min at 30°C, the reaction was terminated by the addition of 4 × SDS sample buffer, and the reaction mixtures were subjected to electrophoresis on 12% SDS-polyacrylamide gels, followed by staining with Coomassie blue, drying, and autoradiography with intensifying screens. In some cases, proteins from cell extracts were subjected to immunoblot analysis using the antibody against the respective MAP kinase to verify their relative expression by enhanced chemiluminescence reaction using a SuperSignal West Pico enhanced chemiluminescence detection kit (Pierce, Rockford, IL).

Statistical Analysis. Data were expressed as means ± S.D., and statistical analysis for multiple comparisons was performed by one-way analysis of variance followed by the Student-Newman-Keuls test. For single comparisons, the significance of difference between means was determined by Student's *t* test. The criterion for statistical significance was $P < 0.05$.

Results

In an initial experiment, PC12 cells were treated with varying concentrations of SAL in the absence or presence of 200 μM Cu^{2+}, and the cell viability was determined by the MTT assay. Although SAL alone caused 26, 41, and 43% of cell death at the concentrations of 125, 250, and 500 μM, respectively, the cytotoxicity of SAL was potentiated by Cu^{2+} (Fig. 2A). Thus, in the presence of 200 μM cupric ion and 125 μM SAL, the viability of cells was reduced to 11% of the control level. Under these experimental conditions, the same concentration of Cu^{2+} did not cause any appreciable cytotoxicity (data not shown). The MTT reduction assay relies on the normal mitochondrial function of viable cells because it determines the activity of succinyl dehydrogenase. We have confirmed the above finding by using the trypan blue-dye exclusion assay (Fig. 2B), which is based on the integrity of intact cellular membranes. The cytotoxicity of SAL was enhanced with increasing concentrations of cupric ion added to the media (Fig. 2C). The copper chelator BCS (Fig. 2D) ameliorated the Cu^{2+}-mediated enhancement of SAL toxicity.

In a subsequent experiment, we examined the morphological changes of PC12 cells incubated with SAL in the absence or presence of Cu^{2+}. Compared with the untreated control PC12 cells (Fig. 3A), cells treated with 100 μM SAL alone became round, and the reflected area was observed in the middle of the treated cells (Fig. 3B), which seemed to be associated with the nuclear condensation indicative of apoptotic cell death. In contrast, cells cotreated with 100 μM SAL and the same concentration of Cu^{2+} aggregated to a large mass (Fig. 3C). Changes in nuclear morphology are also typical of apoptotic cell death. Thus, staining of SAL-treated cells with the nuclear-specific fluorescent dye DAPI revealed condensed and fragmented nuclei of various sizes (Fig. 3E). Such nuclear fragmentation was not evident in control cells (Fig. 3D) or those treated with SAL and copper (Fig. 3F). In situ TUNEL of treated cells also revealed more positive staining in cells exposed to SAL alone (Fig. 3H) than to SAL plus Cu^{2+} (Fig. 3I). Computer-based image analysis of TUNEL-positive cells revealed that SAL treatment alone caused about a 7.3-fold higher apoptotic death rate than did SAL plus Cu^{2+} treatment (i.e., percentage of apoptotic cells, 33.31 ± 9.9 for SAL alone versus 4.59 ± 2.5 for SAL plus Cu^{2+}). Trypan blue and propidium iodide stain only those cells with disrupted plasma membrane integrity; hence, these stains are used in assessing necrotic cell death. PC12 cells exposed to both SAL and Cu^{2+} were stained with trypan blue (Fig. 2B) and propidium iodide (data not shown) to a much greater extent compared with cells treated with SAL alone and untreated control cells. These findings suggest that SAL in combination with cupric ion mainly causes necrotic death in PC12 cells, whereas apoptotic death is more prominent in cells challenged with SAL alone.

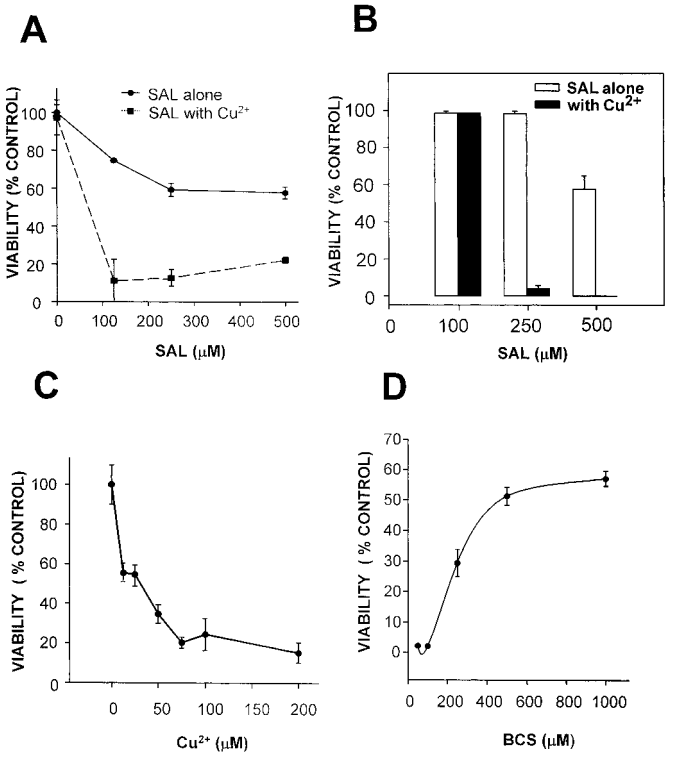

Fig. 2. Cupric ion potentiates SAL-induced PC12 cell death. A, cell viability was assessed by the MTT assay 48 h after treatment with indicated concentrations of SAL in the absence or presence of 200 μM Cu^{2+}. Data are presented as means ± S.E. (n = 4). B, determination of the viability of PC12 cells by the trypan blue exclusion assay after treatment with SAL in the absence or presence of 200 μM Cu^{2+} for 24 h. C, copper-dependent increases in SAL-mediated cytotoxicity. Cells were exposed to 100 μM SAL and varying concentrations of Cu^{2+} for 48 h, and cell viability was measured by the MTT assay. D, protective effects of BCS on SAL- and Cu^{2+}-induced cytotoxicity in cultured PC12 cells. The cell viability was measured as described under A after treatment for 48 h with 250 μM SAL plus the same concentration of Cu^{2+} in the absence or presence of BSC at the indicated concentrations.

Ultrastructural analysis of PC12 cells by transmission electron microscopy was performed to examine the morphological changes at the subcellular level. Although healthy control cells exhibited intact cytoplasmic organelles, well preserved nuclear membranes, and evenly distributed chromatin (Fig. 4A), cells exposed to 100 μM SAL alone showed characteristic chromatin margination at the periphery of the nucleus (Fig. 4B), but there was no substantial changes in cytoplasmic structures. In contrast, PC12 cells subjected to cotreatment with 100 μM Cu^{2+} and the same concentration of SAL exhibited typical ultrastructural features of necrosis, such as extensive membrane and cytoplasmic damages, mitochondrial swelling, etc. (Fig. 4C).

Nonrandom fragmentation of genomic DNA into a ladder of about 180-base-pair nucleosomes has been considered one of the most distinct hallmarks of apoptotic death. To clarify the differential death patterns induced by SAL with and without Cu^{2+}, DNA extracted from PC12 cells treated with 100 μM SAL alone or with SAL plus 100 μM cupric sulfate was analyzed by agarose gel electrophoresis. Interestingly, the ladders of 180 to 200 base pairs, the biochemical hallmark of apoptosis, were seen in DNA from the group treated with SAL alone (Fig. 5A). In the lane loaded with DNA from PC12 cells treated with both 100 μM SAL and the same concentration of copper, DNA was observed as a smear (Fig. 5A), but DNA ladder formation was detected when lower concentrations of Cu^{2+} were added (Fig. 5B). All of the above results, taken together, indicate that cupric ion potentiates the cytotoxic effects of SAL and diverts the SAL-induced death pattern from apoptosis to necrosis.

To examine the possible involvement of ROS in SAL-induced PC12 cell death, we measured the cellular levels of oxidative species accumulated as a result of treatment with SAL or SAL plus copper. Intracellular ROS generation was

monitored by a microfluorescence technique using DCF-DA. PC12 cells exposed to both SAL and cupric ion exhibited substantially increased intracellular accumulation of ROS, as visualized by intense fluorescence derived from DCF-DA (Fig. 6). There was at least 3-fold enhancement of intracellular peroxide formation after challenge with SAL and Cu^{2+} compared with that observed in control cells. However, the identity of oxidative species generated by SAL plus Cu^{2+} remains unknown because DCF-DA detects mainly organic peroxides and hydrogen peroxide, which are permeable to the cellular membrane. The levels of ROS in cells treated with SAL alone were not significantly high compared with those detected in the untreated control cells. SAL alone could conceivably generate ROS also, but this was not detectable at the time point we selected for measurement in this particular experiment. This result implies that Cu^{2+} accelerated redox cycling of SAL and subsequent ROS generation. In agreement with this assumption, SAL alone underwent slow autoxidation in an air-saturated solution, whereas the presence of the same concentration of Cu^{2+} markedly enhanced SAL-induced oxygen consumption (Fig. 7). The addition of antioxidants, such as NAC and GSH, ameliorated the cell death induced by SAL with cupric ion (Table 1). The possible involvement of ROS in SAL-induced PC12 cells death was further confirmed by formation of MDA and 8-oxo-dGuo in treated cells, which are indices of oxidative damage to membrane lipids and cellular DNA, respectively. Treatment with SAL alone caused no substantial increase in the production of MDA compared with untreated control cells, whereas addition of cupric ion significantly increased SAL-induced MDA production (Fig. 8A). Oxidative DNA damage in PC12 cells exposed to SAL with and without Cu^{2+} was detected and quantified by immunocytochemical staining with a monoclonal antibody that specifically recognizes 8-oxo-dGuo (Yarborough et al., 1996). Cells treated with cupric ion alone did not exhibit any significant increases in 8-oxo-dGuo production. Higher levels of specific nuclear staining were observed in cells treated with both SAL and Cu^{2+} compared with those of cells exposed to SAL alone (Fig. 8B). HPLC analysis of 8-oxo-dGuo confirmed the above immunocytochemical data; cells treated with both SAL and Cu^{2+} produced levels of 8-oxo-dGuo approximately 3 times higher compared with those exposed to SAL alone (1.78 for SAL plus Cu^{2+} group versus 0.62 for SAL alone group in terms of 8-oxo-dGuo/10^5 dGuo).

Bcl-2 and Bax are two representative proteins that exert opposite actions in regulating the cell death, particularly

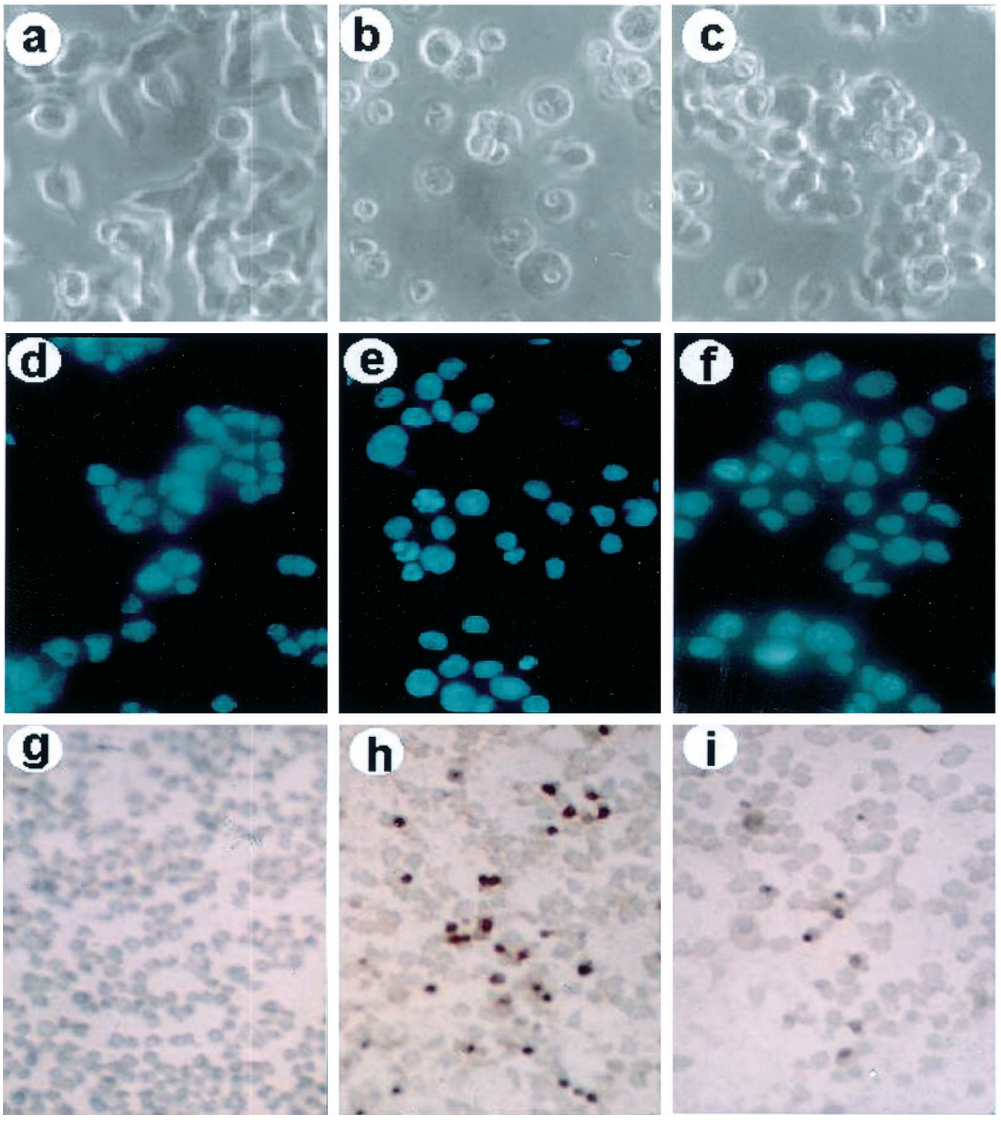

Fig. 3. Microscopic analysis of SAL-mediated cell death with and without copper. Untreated control PC12 cells (A, D, G) or those treated with 100 μM SAL in the absence (B, E, H) or presence (C, F, I) of 100 μM Cu^{2+} for 48 h. A–C, representative phase contrast photographs; D–F, fluorescence image of cells stained with DAPI; G–I, in situ terminal transfer-labeling of cells bearing the 3′ end of fragmented DNA.

apoptosis. Therefore, we have examined the possible involvement of these proteins in mediating apoptosis induced by SAL. Bcl-2 plays a crucial role in cell survival, whereas Bax is considered to be responsible for stimulating cell death. Western blot analysis revealed the increased Bax expression in 4 h after the SAL treatment (Fig. 9A). Because the constitutive level of Bcl-2 was not sufficiently high enough to be detected in PC12 cells (Maroto and Perez-Polo, 1997), the level of Bcl-x_L, which is structurally and functionally analogous to Bcl-2, was alternatively measured by Western blotting in our experiment. The expression of Bcl-x_L was decreased in a time-related manner after SAL treatment (Fig. 9A).

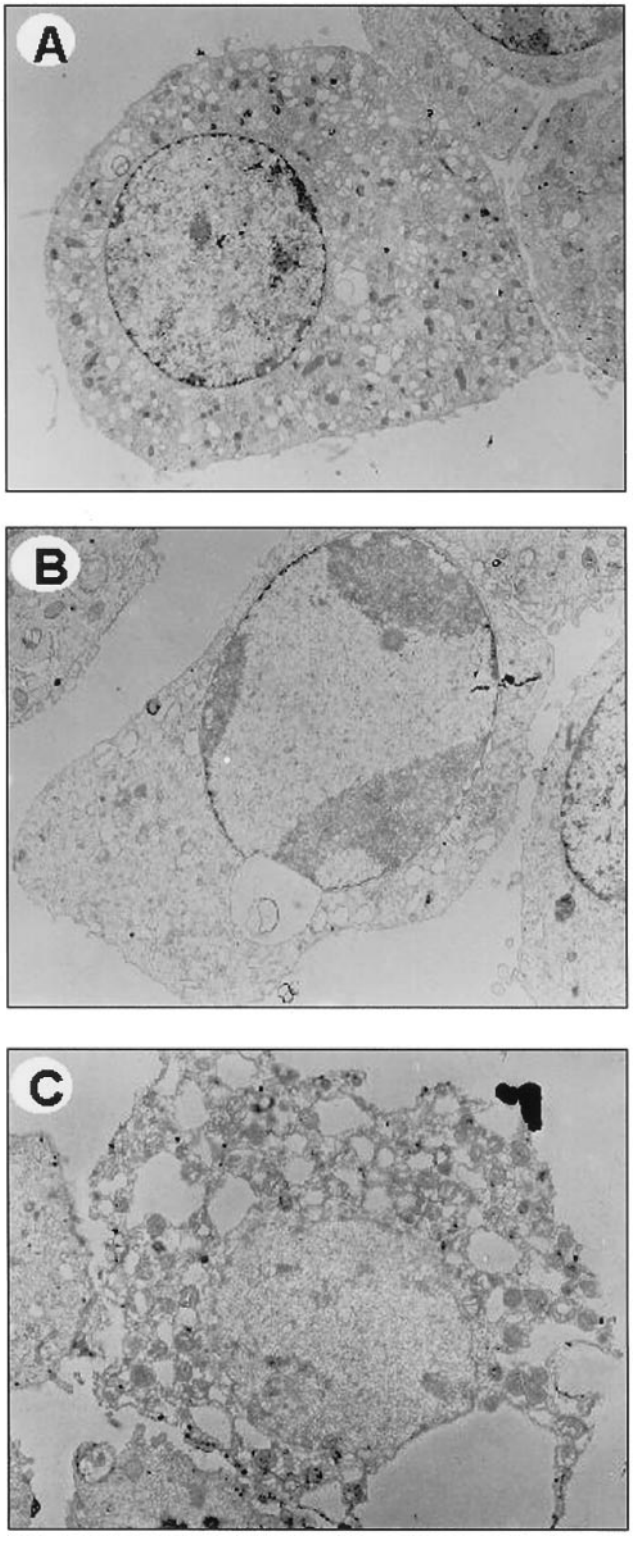

Fig. 4. Transmission electron microscopy of PC12 cells. A, control cells; B, treated with SAL (100 μM); C, treated with SAL (100 μM) and Cu^{2+} (100 μM). Magnification, 3000× (A); 5000× (B and C).

Because Bcl-2 has been reported to have an antioxidant function, it is plausible that this death-suppressing protein is protective against the cell death induced by SAL, which is likely to be mediated by ROS. A stable cell line overexpressing Bcl-2 was used to verify its protective effects on SAL-induced apoptosis. As shown in Fig. 9B, the viability was significantly increased in *bcl-2*-transfected cells compared with vector-transfected control cells after treatment with 250 μM SAL, whereas no substantial protection was observed at other concentrations tested. In addition, PC12 cells transfected with another death-suppressing protein, Bcl-X_L, did not exhibit any appreciable DNA fragmentation when treated with SAL or SAL plus copper (Fig. 9C).

To further investigate the molecular mechanisms underlying SAL-induced apoptosis of PC12 cells, we have examined the effects of SAL on the activities JNK and ERK that are involved in intracellular signal transduction pathways mediating oxidative cell death. Throughout our experiments, comparable amounts of immunoprecipitated kinase proteins and their substrate proteins were always assured by Coomassie blue staining of SDS-polyacrylamide gels and immunoblot analyses using antibodies against the respective proteins. SAL treatment rapidly activated JNK with maximal activation observed at 5 min (Fig. 10). In contrast, the activity of ERK was not affected much by SAL treatment (Fig. 10). These data suggest that SAL is likely to exert its cytotoxic effect in PC12 cells preferentially through activation of the JNK pathway.

Discussion

Tetrahydroisoquinoline alkaloids are found in human fluids and/or tissues (Collins et al., 1979; Adachi et al., 1986; Moser and Kompf, 1992; Rommelspacher et al., 1995; Na-

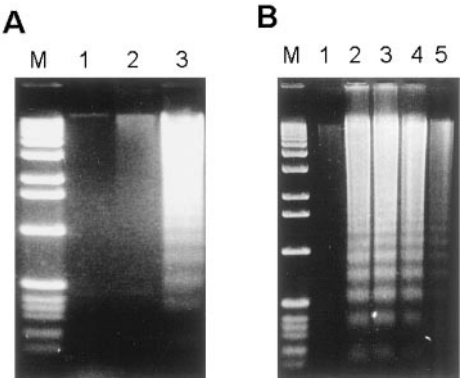

Fig. 5. Analysis of internucleosomal DNA fragmentation in PC12 cells exposed to SAL with and without Cu^{2+}. A, lane 1, control cells; lane 2, treated with SAL (100 μM) and Cu^{2+} (100 μM) for 48 h; lane 3, treated with SAL (100 μM) alone. B, lane 1, control cells; lanes 2 to 5, treated with 100 μM SAL in the absence (lane 2) or presence of 25 μM (lane 3), 50 μM (lane 4), or 100 μM (lane 5) Cu^{2+} for 48 h. Note that DNA ladder formation is more evident with lower concentrations of Cu^{2+}. The first lane in each panel, designated "M", represents a 1-kilobase-pair ladder used as a molecular size marker.

gatsu, 1997). SAL, one of the tetrahydroisoquinoline alkaloids derived from dopamine, is structurally related to 6-OHDA, a prototype catechol neurotoxin that has been known to induce neuronal cell death by generating ROS (Wu et al., 1996). Given the structural similarity to 6-OHDA, SAL is anticipated to cause neurotoxicity via induction of oxidative stress.

Apoptosis is an active, gene-directed, and evolutionarily conserved process from nematodes to mammals. The execution of apoptosis is associated with its characteristic morphological and biochemical changes. In the present study, the SAL-induced PC12 cell death pattern was apoptotic, as determined by various biochemical and morphological features. In the presence of copper, however, the SAL-induced cell death was distinct from that observed with SAL alone. Stimulation of 6-OHDA autoxidation by bivalent copper has been shown to be implicated in neurotoxicity exerted by this catecholamine (Heikkila and Cabbat, 1978). Because SAL has a catechol moiety, it may participate in redox cycling. In the presence of a transition metal such as copper, oxidation of SAL may be facilitated to generate increased amounts of ROS. The ability of SAL to induce DNA damage in vitro was enhanced in the presence of Cu^{2+}, as revealed by an increased proportion of nicked and linear DNA in øX174 or pBR322 DNA (Jung and Surh, 2001), increased 8-oxo-dGuo formation in calf thymus DNA (Jung and Surh, 2001), and also increased tail moment in cultured Chinese hamster lung fibroblast cells (Jung et al., 2001). To support the notion that copper could accelerate the oxidation of SAL and subsequent generation of ROS thereby augmenting oxidative stress, cell death induced by SAL and Cu^{2+} was mitigated by the copper chelator BCS and selected antioxidants, such as NAC and GSH. Furthermore, the amount of ROS produced by SAL with copper was much larger than that generated by SAL alone, as determined by the fluorescent dye DCF-DA, which preferentially detects intracellular peroxides. Cu^{2+} also enhanced oxygen consumption induced by SAL. The significant increase in the formation of MDA and 8-OH-dGuo in PC12 cells treated with both SAL and Cu^{2+} compared with those exposed to SAL alone provides more evidence supporting that copper stimulates SAL-induced ROS generation and oxidative stress by augmenting the redox cycling of SAL. SAL probably forms a complex with Cu^{2+}, leading to its reduction to Cu^{+} with concomitant generation of ROS, as proposed for other catechols or phenolics (Heikkila and Cabbat, 1978; Fazal et al., 1990; Shamsi and Hadi, 1995). Although autoxidation of the catechol moiety may play a role in the PC12 cell death caused by SAL, the presence of other mechanisms that can contribute to SAL-induced cytotoxicity cannot be ruled out. One alternative activation pathway involves the enzymatic *N*-methylation of SAL. The *N*-methylated metabolite of SAL induced DNA damage and apoptosis in cultured human neuroblastoma SH-SY5Y cells (Maruyama et al., 1997; Akao et al., 1999). The *N*-methyl-(*R*)-SAL-induced apoptosis seems to be mediated through activation of caspase-3 (Akao et al., 1999). Inhibition of mitochondrial respiration and ATP synthesis by tetrahydroisoquinoline-like endogenous alkaloids structurally related to SAL has been mediated by inhibition of complex I in the respiratory chain (Suzuki et al., 1990). Dehydrogenation of SAL will produce dihydroisoquinoline, which can form extremely electrophilic tautomers capable of damaging critical cellular macromolecules (e.g., membrane lipids, proteins, nucleic acids, etc.), which may also account for SAL-mediated cytotoxicity, as suggested by Collins (1982).

Interestingly, the type of cell death induced by SAL plus copper was necrotic, as characterized by cytoplasmic damage, mitochondrial swelling, and plasma membrane damage. Such differential cell death patterns seem to be attributable to the larger amounts of ROS generated by SAL in the pres-

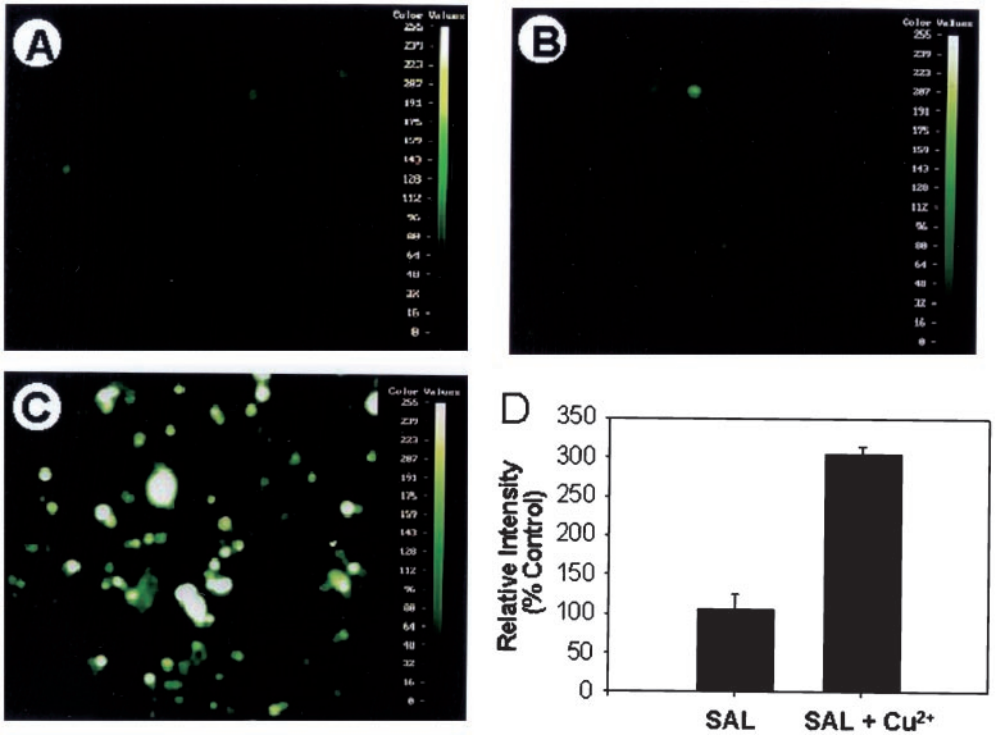

Fig. 6. Comparative intracellular accumulation of ROS in PC12 cells. After 90 min of incubation, the amounts of peroxide were measured with the use of the fluorescent dye DCF-DA, as described under *Experimental Procedures*. A, control cells; B, treated with SAL (100 μM) alone; C, treated with SAL (100 μM) plus Cu^{2+} (100 μM); D, quantification of peroxide accumulation.

ence of copper, thereby causing more extensive oxidative stress toward the exposed cells. Oxidant-induced cell death mediated by way of necrosis is distinct from that induced via apoptosis, and the intensity of the oxidative stress may determine which pathway is triggered. Gardner et al. (1997) reported that cells exposed to high concentrations of hydrogen peroxide seemed to die through necrosis, whereas lower concentrations induced apoptotic death. Because SAL produced more ROS in the presence of copper, the cell death pattern might have been switched from apoptosis to necrosis. Furthermore, DNA ladder formation was evident in our study when PC12 cells were incubated with SAL and relatively low concentrations of Cu^{2+}, whereas DNA from cells treated with higher concentrations of Cu^{2+} along with SAL looked like a smear on the agarose gel electrophoresis, reflecting necrotic death.

The role of JNK in apoptosis is controversial. In some cells, such as those from c-Fos or c-Jun null embryos (Roffler-Tarlov et al., 1996) and sympathetic motor neurons (Virdee et al., 1997), JNK activation or phosphorylated c-Jun may not be a causal factor in apoptosis. On the other hand, in other types of cells, like PC12 cells, JNK activation is associated with apoptosis because activation of AP-1 activity and over-expression of c-Jun, SEK1, or ASK1 proteins led to cell death (Ichijo et al., 1997; Luo et al., 1998; Soh et al., 2000) or counteracted the antiapoptotic effect of Bcl-2 (Park et al., 1997). JNK is required for apoptosis of primary murine em-

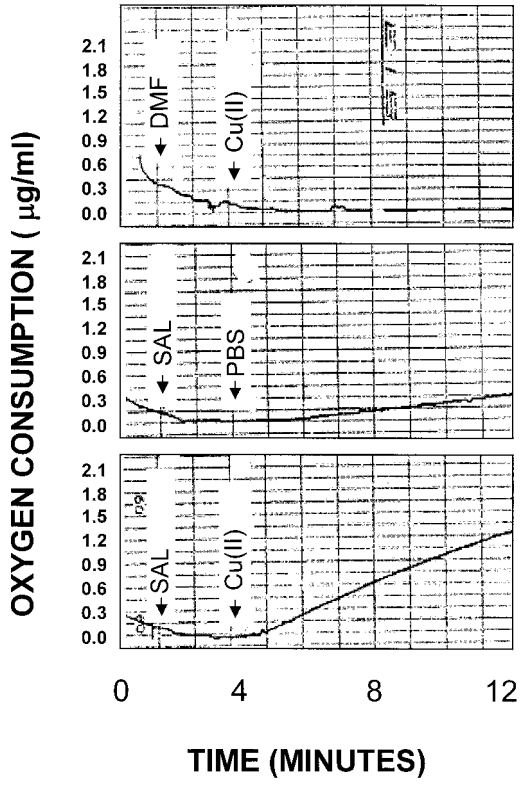

Fig. 7. Comparison of oxygen consumption in reaction mixtures containing Cu^{2+} alone (upper panel), SAL alone (middle panel), or both (lower panel). Reaction mixtures contained Cu^{2+} (250 μM), SAL (250 μM), or both in PBS. Oxygen consumption was recorded continuously for 12 min at room temperature with a Clark O_2 electrode.

TABLE 1

Protective effects of NAC and GSH on PC12 cell death induced by SAL plus copper

Cell viability was determined by the MTT assay 30 h after the treatment with SAL (250 μM or 500 μM) and Cu^{2+} (100 μM) in the presence or absence of antioxidants. The concentration of each antioxidant was 1 mM.

SAL	Antioxidant	Viability
μM		*% of control*
250		42.0 ± 7.25
	NAC	73.9 ± 2.37[a]
	GSH	69.3 ± 8.42[a]
500		9.3 ± 3.29
	NAC	50.6 ± 9.20[a]
	GSH	47.6 ± 8.15[a]

[a] Significantly different from the value obtained with SAL alone treatment ($P < 0.01$).

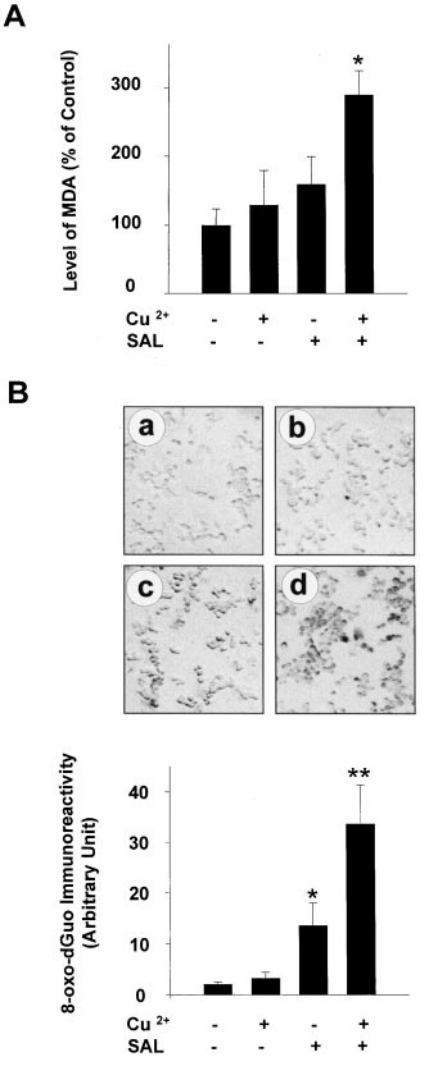

Fig. 8. Comparison of oxidative damage to membrane lipid (A) and DNA (B) induced by SAL or SAL plus Cu^{2+}. PC12 cells were exposed to 100 μM SAL alone or 100 μM SAL plus Cu^{2+} at 37°C for 24 h. A, lipid peroxidation was determined by measuring the levels of MDA. The data are the means ± S.D. expressed as percentage of the untreated control value (n = 3). The average amount of MDA in untreated control cells was 0.537 ± 0.14 nmol/mg of protein. Analysis of variance was followed by the Student-Newman-Keuls test for post hoc comparison. *, significantly different from the other groups ($P < 0.05$). B, 8-oxo-dGuo was detected and quantified by the immunoperoxidase method, as described under *Experimental Procedures*; a, untreated control cells; b, treated with Cu^{2+} alone; c, treated with SAL alone; d, treated with both Cu^{2+} and SAL. Asterisks indicate significant differences from the control group (*$P < 0.05$) or all the other groups (**$P < 0.001$).

bryonic fibroblasts by mediating cytochrome *c* release from mitochondria (Tournier et al., 2000). Conversely, neuronal cell death via apoptosis was blocked by a novel inhibitor of the JNK-signaling pathway (Maroney et al., 1998) or by c-Jun-dominant negative mutant (Ham et al., 1995). A synthetic chemopreventive agent, *N*-(4-hydroxyphenyl)retinamide, causes apoptosis in the LNCaP cell line, whereas it was inactive in another prostate cancer cell line, PC-3 cells (Chen et al., 1999). Therefore, whether JNK activation is a prerequisite for cell death seems to depend on the cell type, cell death signal, the duration of JNK activation, and the intracellular environment. In the case of PC12 cells, JNK activation seems to be an early event for apoptosis by ceramide (Hartfield et al., 1998), 4-hydroxynonenal (Soh et al., 2000), and withdrawal of survival factors (Le-Niculescu et al., 1999). The rapid activation of JNK in PC12 cells after exposure to SAL suggests the proapoptotic function of this stress-activated protein kinase, which is in agreement with the aforementioned findings by other investigators. In contrast to JNK, ERK has been proposed to exert an opposite role in apoptosis. Thus, withdrawal of nerve growth factor led to inhibition of ERK with concomitant activation of JNK and p38 MAP kinase (Xia et al., 1995). However, we have not found any noticeable decrease in the ERK activation in SAL-treated PC12 cells.

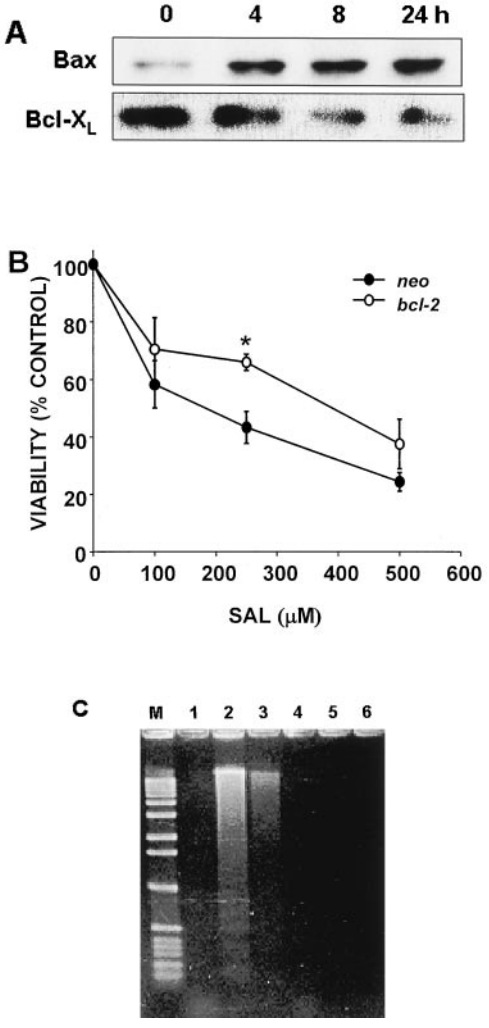

Fig. 9. Western blot analysis of Bax and Bcl-x_L expression in SAL-treated PC12 cells. A, cells were treated with 100 μM SAL and harvested at indicated times for immunoblot analysis with anti-Bax and anti-Bcl-x_L. B, comparison of viability of PC12 cells transfected with *bcl-2* (○) or the empty vector alone (●). C, internucleosomal DNA fragmentation in vector-transfected (lanes 1–3) and *bcl-x_L*-overexpressing (lanes 4–6) PC12 cells. Cells were treated with 0 μM (lanes 1 and 4) or 100 μM SAL in the absence (lanes 2 and 5) or presence of 100 μM Cu^{2+} (lanes 3 and 6) for 48 h. M represents 1 kilobase pair ladder used as a molecular marker.

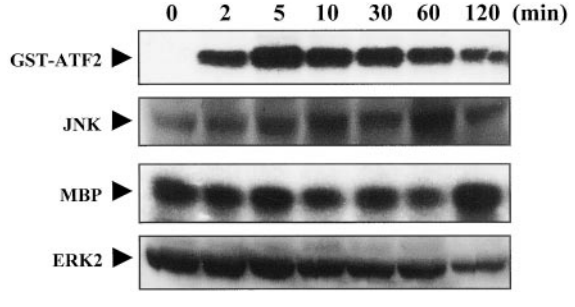

Fig. 10. Effects of SAL on activation of JNK and ERK2 in PC12 cells. Cells were treated with 100 μM SAL and JNK, and ERK activities were determined at the indicated times using glutathione *S*-transferase activating transcription factor-2 fusion protein and myelin basic protein as substrates, respectively. The incubation conditions and other details are described under *Experimental Procedures*.

Bcl-2 that resides in mitochondrial, microsomal, and nuclear membrane sites regulates apoptosis via the formation of a homodimer or a heterodimer with the death-stimulating protein Bax. According to current hypotheses, control of oxidative stress may be common elements through which Bcl-2 exerts its survival function. SAL treatment to PC12 cells resulted in reduced expression of Bcl-x_L protein, which is structurally and functionally analogous to Bcl-2. Our present study also reveals that transfection of PC12 cells with this antiapoptotic protein blocks DNA fragmentation induced by SAL. In addition, the cytotoxicity of SAL was apparently reduced in Bcl-2 overexpressing PC12 cells. The protective effects of Bcl-2 against oxidative stress induced by several stimuli are well known. For instance, treatment of cells with hydrogen peroxide, *tert*-butylhydroperoxide, menadione, and the GSH synthesis inhibitor buthionine sulfoximine led to cell death, which was efficiently blocked by *bcl-2* overexpression (Hockenbery et al., 1993). The attenuation of SAL-induced toxicity in PC12 cells overexpressing *bcl-2* may provide further evidence supporting that oxidative stress is implicated in the cell death caused by this neurotoxic catechol. Additional studies will be required to elucidate the intracellular signaling cascades that mediate the SAL-induced cell death via oxidative stress.

Acknowledgments

We are grateful to Prof. Sang Dai Park and Prof. Seung Hwan Hong of the Institute for Molecular Biology of Seoul National University for providing the facilities for electromicroscopy, and Young-Ho Ahn for excellent technical support. We thank Jung-Hwan Kim of the College of Pharmacy, Seoul National University, for illustration work.

References

Adachi J, Mizol Y and Fukunaga T (1986) Individual difference in urinary excretion of salsolinol in alcoholic patients. *Alcohol* **3:**371–376.

Akao Y, Nakagawa Y, Maruyama W, Takahashi T and Naoi M (1999) Apoptosis induced by an endogenous neurotoxin, *N*-methyl(*R*)salsolinol, is mediated by activation of caspase 3. *Neurosci Lett* **267:**153–156.

Bryan SF, Vizard DC, Beary DA, LaBiche RA and Hardy KJ (1981) Partitioning of zinc and copper within subnuclear nucleoprotein particles. *Nucleic Acid Res* **9:**5811–5823.

Chen Y-R, Zhou G and Tan T-H (1999) c-Jun *N*-terminal kinase mediates apoptotic

signaling induced by *N*-(4-hydroxyphenyl)retinamide. *Mol Pharmacol* **56:**1271–1279.
Collins MA (1982) A possible neurochemical mechanism for brain and nerve damage associated with chronic alcoholism. *Trends Pharmacol Sci* **3:**373–375.
Collins MA, Nijm WP, Borge GF, Teas G and Goldfarb C (1979) Dopamine-related tetrahydroisoquinoline: significant urinary excretion by alcoholics after alcohol consumption. *Science (Wash DC)* **206:**1184–1186.
Fazal F, Rahman A, Greensill J, Ainley K, Hadi SM and Parish JH (1990) Strand scission in DNA by quercetin and Cu (II): identification of free radical intermediates and biological consequence of scission. *Carcinogenesis* **11:**2005–2008.
Gardner AM, Xu FH, Fady C, Jacoby FJ, Duffey DC, Tu Y and Lichtenstein A (1997) Apoptotic vs. nonapoptotic cytotoxicity induced by hydrogen peroxide. *Free Radic Biol Med* **22:**73–83.
Graham DG, Tiffany SM, Bell WR Jr and Gutknecht WF (1978) Autoxidation versus covalent binding of quinones as the mechanism of toxicity of dopamine, 6-hydroxydopamine, and related compounds toward C1300 neuroblastoma cells in vitro. *Mol Pharmacol* **14:**644–653.
Haber H, Winkler A, Putscher I, Henklein P, Baeger I, Georgi M and Melzig MF (1996) Plasma and urine salsolinol in humans: effect of acute ethanol intake on the enantiomeric composition of salsolinol. *Alcoholism Clin Exp Res* **20:**87–92.
Ham J, Babij C, Whitfield J, Pfarr CM, Lallemand D, Yaniv M and Rubin LL (1995) A c-Jun dominant negative mutant protects sympathetic neurons against programmed cell death. *Neuron* **14:**927–939.
Hartfield PJ, Bilney AJ and Murray AW (1998) Neurotrophic factors prevent ceramide-induced apoptosis downstream of c-Jun *N*-terminal kinase activation in PC12 cells. *J Neurochem* **71:**161–169.
Heikkila RE and Cabbat FS (1978) The stimulation of 6-hydroxydopamine autoxidation by bivalent copper: potential importance in the neurotoxic process. *Life Sci* **23:**33–38.
Hockenbery DM, Oltvai ZN, Yin X-M, Milliman CL and Korsmeyer SJ (1993) Bcl-2 functions in an antioxidant pathway to prevent apoptosis. *Cell* **74:**241–251.
Ichijo H, Nishida E, Irie K, ten Dijke P, Saitoh M, Moriguchi T, Takagi M, Matsumoto K, Miyazono K and Gotoh Y (1997) Induction of apoptosis by ASK1, a mammalian MAPKKK that activates SAPK/JNK and p38 signaling pathways. *Science (Wash DC)* **275:**90–94.
Jung Y-J and Surh Y-J (2001) Oxidative DNA damage and cytotoxicity induced by copper-stimulated redox cycling of salsolinol, a neurotoxic tetrahydroisoquinoline alkaloid. *Free Radic Biol Med* **30:**1407–1417.
Jung Y-J, Youn J-Y, Ryu J-C and Surh Y-J (2001) Salsolinol, a naturally occurring tetrahydroisoquinoline alkaloid, induces DNA damage and chromosomal aberrations in cultured Chinese hamster lung fibroblast cells. *Mutat Res* **474:**25–33.
Kim H-J, Yoon H-R, Washington S, Chang II, Oh YJ and Surh Y-J (1997) DNA strand scission and PC12 cell death induced by salsolinol and copper. *Neurosci Lett* **238:**95–98.
Le-Niculescu H, Bonfoco E. Kasuya Y, Claret FX, Green DR and Karin M (1999) (1999) Withdrawal of survival factors results in activation of the JNK pathway in neuronal cells leading to Fas ligand induction and cell death. *Mol Cell Biol* **19:**751–763.
Levay G, Ye Q and Bodell WJ (1997) Formation of DNA adducts and oxidative base damage by copper mediated oxidation of dopamine and 6-hydroxydopamine. *Exp Neurol* **146:**570–574.
Li Y, Trush A and Yager JD (1994) DNA damage caused by reactive oxygen species originating from a copper-dependent oxidation of 2-hydroxy catechol of estradiol. *Carcinogenesis* **15:**1421–1427.
Luo Y, Umegaki H, Wang X, Abe R and Roth GS (1998) Dopamine induces apoptosis through an oxidation-involved SAPK/JNK activation pathway. *J Biol Chem* **273:**3756–3764.
Maroney AC, Glicksman MA, Basma AN, Walton KM, Knight E Jr, Murphy CA, Bartlett BA, Finn JP, Angeles T. Matsuda Y, et al. (1998) Motor neuron apoptosis is blocked by CEP-1347 (KT 7515), a novel inhibitor of the JNK signaling pathway. *J Neurosci* **18:**104–111.
Maroto R and Perez-Polo JR (1997) Bcl-2-related protein expression in apoptosis: oxidative stress versus serum deprivation in PC12 cells. *J Neurochem* **69:**514–523.
Maruyama W, Naoi M, Kasamatsu T, Hashizume Y, Takahashi T, Kohda K and Dostert P (1997) An endogenous dopaminergic neurotoxin, *N*-methyl-(*R*)-salsolinol, induces DNA damage in human dopaminergic neuroblastoma SH-SY5Y cells. *J Neurochem* **69:**322–329.
Moser A and Kompf D (1992) Presence of methyl-6,7-dihydroxy-1,2,3,6-tetrahydroisoquinolines, derivatives of the neurotoxin isoquinoline, in parkinsonian lumbar CSF. *Life Sci* **50:**1885–1891.
Myers WD, Mackenzie L, Ng KT, Singer G, Smythe GA and Duncan MW (1985) Salsolinol and dopamine in rat medial basal hypothalamus after chronic ethanol exposure. *Life Sci* **36:**309–314.
Nagatsu T (1997) Isoquinoline neurotoxins in the brain and Parkinson's disease. *Neurosci Res* **29:**99–111.
Nakayama T, Terazaura K and Kawakishi S (1992) Cytotoxicity of glucosone in the presence of cupric ion. *J Agric Food Chem* **40:**830–833.
Nappi AJ and Vass E (1994) The effects of glutathione and ascorbic acid on the oxidation of 6-hydroxydopa and 6-hydroxydopamine. *Biochim Biophys Acta* **1201:**498–504.
Park J, Kim I, Oh Y. J, Lee, Han PL and Choi EJ (1997) Activation of c-Jun *N*-terminal kinase antagonizes an anti-apoptotic action of Bcl-2. *J Biol Chem* **272:**16725–16728.
Roffler-Tarlov S, Brown JJ, Tarlov E, Stolarov J, Chapman DL, Alexiou M and Papaioannou VE (1996) Programmed cell death in the absence of c-Fos and c-Jun. *Development* **122:**1–9.
Rommelspacher H, Baum SS, Dufeu P and Schmidt LG (1995) Determination of (*R*)- and (*S*)-salsolinol sulfate and dopamine sulfate levels in plasma of nonalcoholics and alcoholics. *Alcohol* **12:**309–315.
Shamsi FA and Hadi SM (1995) Photoinduction of strand scission in DNA by uric acid and Cu (II). *Free Radic Biol Med* **19:**189–196.
Soh Y, Jeong K-S, Lee IJ, Bae M-A, Kim Y-C and Song BJ (2000) Selective Activation of the c-Jun *N*-terminal protein kinase pathway during 4-hydroxynonenal-induced apoptosis of PC12 Cells. *Mol Pharmacol* **58:**535–541.
Suzuki K, Mizuno Y and Yoshida M (1990) Inhibition of mitochondrial respiration by 1,2,3,4-tetrahydroisoquinoline-like endogenous alkaloids in mouse brain. *Neurochem Res* **15:**705–710.
Tournier C, Hess P, Yang DD, Xu J, Turner T, Nimnual A, Bar-Sagi D, Jones SN, Flavell RA and Davis RJ (2000) Requirement of JNK for stress-induced activation of the cytochrome c-mediated death pathway. *Science (Wash DC)* **288:**870–874.
Virdee K, Bannister AJ, Hunt SP, Tolkovsky AM (1997) Comparison between the timing of JNK activation, c-Jun phosphorylation, and onset of death commitment in sympathetic neurones. *J Neurochem* **69:**550–561.
Wu Y, Blum D, Nissou M-F, Benabid A-L and Verna J-M (1996) Unlike MPP+, apoptosis induced by 6-OHDA in PC12 cell is independent of mitochondrial inhibition. *Neurosci Lett* **221:**69–71.
Xia Z, Dickens M, Raingeaud J, Davis RJ and Greenberg ME (1995) Opposing effects of ERK and JNK-p38 MAP kinases on apoptosis. *Science (Wash DC)* **270:**1326–1331.
Yarborough A, Zhang Y-J, Hsu T-M and Santella RM (1996) Immunoperoxidase detection of 8-hydroxydeoxyguanosine in aflatoxin B_1-treated rat liver human oral mucosal cells. *Cancer Res* **56:**683–688.

Address correspondence to: Professor Young-Joon Surh, College of Pharmacy, Seoul National University, Shinlim-dong, Kwanak-gu, Seoul 151-742, Korea. E-mail: surh@plaza.snu.ac.kr